

T-wave morphology can distinguish healthy controls from LQTS patients

S A Immanuel^{1,2,5}, A Sadrieh^{1,5}, M Baumert², J P Couderc³,
W Zareba³, A P Hill^{1,4} and J I Vandenberg^{1,4}

¹ Mark Cowley Lidwill Research Program in Cardiac Electrophysiology,
Victor Chang Cardiac Research Institute, Sydney, Australia

² Department of Electrical and Electronics Engineering, University of Adelaide,
Adelaide, Australia

³ Heart Failure Follow up Program, University of Rochester Medical College,
Rochester, USA

⁴ St Vincent's Clinical School, University of NSW, Sydney, Australia

E-mail: j.vandenberg@victorchang.edu.au

Received 20 May 2016, revised 24 June 2016

Accepted for publication 20 July 2016

Published 11 August 2016



CrossMark

Abstract

Long QT syndrome (LQTS) is an inherited disorder associated with prolongation of the QT/QTc interval on the surface electrocardiogram (ECG) and a markedly increased risk of sudden cardiac death due to cardiac arrhythmias. Up to 25% of genotype-positive LQTS patients have QT/QTc intervals in the normal range. These patients are, however, still at increased risk of life-threatening events compared to their genotype-negative siblings. Previous studies have shown that analysis of T-wave morphology may enhance discrimination between control and LQTS patients. In this study we tested the hypothesis that automated analysis of T-wave morphology from Holter ECG recordings could distinguish between control and LQTS patients with QTc values in the range 400–450 ms. Holter ECGs were obtained from the Telemetric and Holter ECG Warehouse (THEW) database. Frequency binned averaged ECG waveforms were obtained and extracted T-waves were fitted with a combination of 3 sigmoid functions (upslope, downslope and switch) or two 9th order polynomial functions (upslope and downslope). Neural network classifiers, based on parameters obtained from the sigmoid or polynomial fits to the 1 Hz and 1.3 Hz ECG waveforms, were able to achieve up to 92% discrimination between control and LQTS patients and 88% discrimination between LQTS1 and LQTS2 patients. When we analysed a subgroup of subjects with normal QT intervals (400–450 ms, 67 controls and 61 LQTS), T-wave morphology based parameters enabled 90% discrimination

⁵The authors contributed equally to this work.

between control and LQTS patients, compared to only 71% when the groups were classified based on QTc alone. In summary, our Holter ECG analysis algorithms demonstrate the feasibility of using automated analysis of T-wave morphology to distinguish LQTS patients, even those with normal QTc, from healthy controls.

Keywords: cardiac arrhythmia, sudden cardiac death, long QT syndrome, Holter ECG, T-wave morphology, neural network classifier

 Online supplementary data available from stacks.iop.org/PM/37/1456/mmedia

(Some figures may appear in colour only in the online journal)

1. Introduction

The pumping activity of the heart is controlled by a high fidelity electrical signalling system that ensures the co-ordinated contraction and relaxation of the heart muscle. The surface electrocardiogram (ECG) provides a non-invasive means of monitoring these electrical signals, and as such has been an invaluable clinical diagnostic tool for over 100 years (Rosen 2002). The resting ECG, which is typically recorded over 3–4 cardiac cycles, provides a snapshot of the status of the heart. Alternatively, a Holter ECG can provide insights into the dynamics of cardiac electrical activity during a 24 h period (Zareba and De Luna 2005) to the large computational demands required for processing and analysing the amounts of data that can be recorded (of the order of 100 000 beats per 24 h), until recently the clinical application of Holter ECG recordings have been largely limited to detecting arrhythmic episodes and/or ectopic beats (Mauriello *et al* 2011, Katriotis *et al* 2013) and assessing heart rate variability (Task Force of The European Society of Cardiology and The North American Society of Pacing and Electrophysiology 1996). However, there is widespread recognition that there is a wealth of information related to dynamics of depolarization and repolarization contained within Holter ECG recordings that could also have significant clinical utility (Baumert 2016, Baumert *et al* 2016).

Congenital long QT syndrome (LQTS) is an autosomal dominant condition caused by mutations in genes that encode for cardiac ion channels or proteins that regulate their activity. There are at least 16 different genetic subtypes of LQTS, however the majority of patients have mutations in one of two potassium channel genes; mutations in *KCNQ1* (LQTS1) account for ~35% of all LQTS patients and mutations in *KCNH2* (LQTS2) account for ~30% of all LQTS patients (Splawski *et al* 2000). LQTS is characterised by delayed cardiac repolarization, which manifests as prolongation of the QT interval on the surface electrocardiogram (ECG) and results in a markedly increased risk of sudden cardiac death (Moss and Schwartz 2005). The natural history of LQTS can range from death *in utero*, to sudden death in the young, occasional syncopal episodes to an asymptomatic course well into adulthood. Patients with mild disease can be adequately managed with drug therapy (Vincent 2005) whereas patients with severe disease warrant prophylactic treatment with an implantable cardiac defibrillator (Zipes *et al* 2006). The critical question then is how to predict in advance those patients who are at greatest risk of a lethal cardiac arrhythmia. To complicate matters further, whilst prolongation of the QTc interval on the surface electrocardiogram (ECG) is the pathognomonic feature of LQTS, there is tremendous overlap between the QTc intervals of 'normal population' and genotype positive LQTS patients (Goldenberg *et al* 2011). Subjects with greatly prolonged

Table 1. Summary of patient group included in final analyses.

	Control	LQTS1	LQTS2
Age (yrs) ^a (mean ± SD)	35.6 ± 14.6	28.2 ± 17.7	28.6 ± 18.7
Gender	75F/65M	78F/55M	29F/32M
Beta blocker (<i>n</i> , %)	(0, 0%)	(36, 27%)	(23, 38%)

^aOne subject in control, one in LQTS1 and one in LQTS2—no age entry.

QTc intervals on their ECG who present with syncopal episodes are easy to diagnose but those with no overt symptoms and only mildly prolonged or normal range QTc may escape detection. Furthermore, QT interval is modified by heart rate and so a snapshot measurement of QT on a resting ECG may miss a potentially prolonged QTc interval (Page *et al* 2016). Thus measurement of QTc interval alone is an inadequate screening tool. Furthermore, whilst a markedly prolonged QTc interval is associated with greater risk of sudden death (Goldenberg *et al* 2008) it is not an adequate marker for identification of patients at high risk of sudden death.

The QT interval is just one measure of the repolarization properties of the heart and recently there has been considerable interest in looking at whether additional measures of repolarization could assist with deeper phenotyping of patients with long QT syndrome (Page *et al* 2016). For example, there is good empirical evidence that LQTS patients have altered T-wave morphology (Lehmann *et al* 1994) and that there are distinct differences between the different LQTS subtypes. For example, LQTS1 patients typically show broad tall T-waves whilst LQTS2 patients typically show low amplitude and often bifid T-waves (Moss and Robinson 1992). The challenge now is to develop tools to convert these observations into quantifiable parameters that they can be used to more fully characterize the repolarization phenotypes of patients. Previous attempts to quantify repolarization morphology included T-wave modeling approaches (Padrini *et al* 1995, Kanters *et al* 2004, Badilini *et al* 2008), quantification of the time and amplitude distribution across the T-wave (Zareba *et al* 2000, Couderc *et al* 2003, Vaglio *et al* 2008), measurement of changes in the morphology of the T-loop (Zabel *et al* 2002), and ratio of the upslope to downslope of the T-wave (Couderc *et al* 2006, Bhuiyan *et al* 2015). These studies however have largely relied on manual measurements or semi-automated analysis of digitized ECG signals. Furthermore, most of these studies have been largely restricted to analysis of resting ECGs and so have not incorporated dynamic changes such as those associated with changes in heart rate.

In this study, we sought to develop computer algorithms for quantifying the T-wave morphology of ECG tracings recorded at different heart rates. We then used these tools to test the hypothesis that addition of T-wave morphology biomarkers could improve discrimination between control and LQTS patients as well as between subtypes of LQTS patients. We also, show that the addition of T-wave morphology biomarkers can greatly improve the detection of genotype-positive LQTS patients with normal QT intervals.

2. Methods

2.1. Study population

Holter ECG records (with de-identified patient details), along with their cardiac beat annotation information, were obtained from the THEW database (Couderc 2010) for subjects in three groups: Controls, LQTS1 and LQTS2. Demographics of patients that were included in the final analysis are summarized in table 1. Recordings were digitized at 200 Hz. Where there

were multiple recordings for the same patient we chose the earliest recording for adult patients whereas for children we chose the most recent recording that was made prior to commencement of β -blockers.

2.2. ECG processing and measurements

Recordings from lead I, which had upright T-waves (Controls, 159; LQTS1, 171; LQTS2, 89) were processed through automated routines developed using signal processing toolbox in MATLAB environment. Heart beats were grouped into six bins according to the beat frequency in Hz. The six bins contained beats that fell within the range 0.875–0.925, 0.975–1.025, 1.075–1.125, 1.175–1.225, 1.275–1.325, 1.375–1.425 Hz. For simplicity each bin is referred to by its central frequency (0.9, 1.0, 1.1, 1.2, 1.3, 1.4 Hz). Further, we filtered bins based on R-wave amplitude and RR interval of the subsequent beat. This was done to exclude outliers, ectopic beats and beats with abnormally short or long coupling with subsequent beats, as previously described (Hodkinson *et al* 2016). Average ECG curves from within each bin were extracted, with a criterion that at least 100 beats had to be included to qualify for averaging. The technique called RR bin analysis allows for controlling the effect of heart rate on repolarization measurements (Badilini *et al* 1999).

2.2.1. Fiducial points. Beat to beat R peak locations were extracted from the cardiac annotation information made available in the THEW database. To detect Qstart, we analysed the differentiated ECG signal in the 60ms preceding the R peak. The T-P interval was used to define the isoelectric line according to standard practice (Goldenberg *et al* 2006). The end of the T wave was defined as the intercept of an isoelectric level and a line tangential to the point of maximum T wave down slope. Fiducial points corresponding to Q, R, peak of T wave and end of the T-wave were confirmed by visual inspection by two independent investigators (JV & SI). If the automatically picked fiducial points did not correspond (within ~20ms) to the manually picked points, the averaged ECG trace was discarded from the analysis. The number of subjects for which averaged ECGs at each frequency bin satisfied both the minimum criterion of 100 beats and passed visual inspection tests are summarized in supplementary table 1 (stacks.iop.org/PM/37/1456/mmedia).

2.2.2. Curve fitting. To extract the T wave segment for fitting with sigmoidal and polynomial functions, a peak search algorithm was applied to the post-QRS segment of the average curves to locate peak of T wave (T_p). From this point, the start of the T wave segment for curve fitting was defined as a point midway between the peak of the R wave (R_p) and T_p and the end of the T wave segment for curve fitting was set an equivalent time after T_p .

This T-wave segment was fitted with a combination of three Boltzmann sigmoidal functions (upslope, downslope and switch) given by the general expression

$$y = \frac{A_1 - A_2}{1 + e^{\pm \frac{(x_0 - x)}{\tau}}} + A_2 \quad (1)$$

where A_1 and A_2 are the magnitudes at the start and the end of each segment, x_0 is the time point at mid value between A_1 and A_2 and tau are the time constants corresponding to each of the upslope (tau1), switch (tau3) and the downslope (tau2) segments of the T wave, with negative sign on the exponent being applied during the downslope sigmoidal fitting (see figure 2 below). The T wave segments were also fitted with two 9th order polynomial functions, one for the upslope and one for the downslope and the fitting coefficients were determined:

Table 2. ECG parameters analyzed in this study.

Conventional parameters	
Q_T	Q to T end (tangent) (ms)
T_pT_e	T peak to T end (ms)
T_h	Height of T peak (μV)
Sigmoid fit based parameters	
sig_int	Sigmoid intercept point (ms)
tau1	Time constant for sigmoid fit of T wave upslope (ms)
tau2	Time constant for sigmoid fit of T wave downslope (ms)
tau3	Time constant for sigmoid fit of T wave switch (ms)
Polynomial fit based parameters	
Max_loc	Location of T peak (ms)
U_0 to U_9	Polynomial fitting coefficients for upslope of T wave
D_0 to D_9	Polynomial fitting coefficients for downslope of T wave

$$\text{upslope} = U_0 + U_1 \cdot t + U_2 \cdot t^2 + \dots U_9 \cdot t^9 \tag{2}$$

$$\text{downslope} = D_0 + D_1 \cdot t + D_2 \cdot t^2 + \dots D_9 \cdot t^9 \tag{3}$$

where U_0 to U_9 and D_0 to D_9 are the respective coefficients for the up and down slope polynomial fits (see figure 3 below). A summary of all parameters derived from the fitting procedures are summarised in table 2.

2.3. Neural network classifiers

To investigate whether the extracted T-wave morphology markers could improve diagnostic classification of LQTS versus control and between LQTS subtypes we used a neural network classifier approach and compared their performance when based on conventional parameters to those based on parameters derived from different fitting techniques. We used the MATLAB neural network toolbox where the Levenberg–Marquardt back-propagation training algorithm was used to train a multilayer (8-layered) perceptron neural network using the mean square error performance function. Classifiers were derived for (i) Control versus LQTS and (ii) LQTS1 versus LQTS2. In both classifiers, the aim is to assign the input subjects to one of two classes, so that they represent the probability of class membership. Parameters derived from ECG curves averaged within each frequency bin were fed in three groups (i) Conventional (ii) Sigmoid fit based (iii) Polynomial fit based. Each classifier was run 100 times with subject data during each run randomly divided and assigned: 70% for training the network, 15% for testing and 15% for validation of the network. Classification results of the neural networks are presented as example ROC curves and average data presented in confusion matrices.

2.4. Statistical analysis

Data were analyzed with the Prism software package (GraphPad Software Inc., San Diego CA) version 5.01 for Windows (Microsoft, Washington, USA). One-way analysis of variance (ANOVA) and *post hoc* multiple comparisons using Tukey method were used to compare (i) distribution of parameters between groups within each frequency bin and (ii) neural network discrimination between groups based on conventional, sigmoid or polynomial fitting

parameters within frequency bins (iii) neural network discrimination between frequency bins within each parameter group. Student *t* test was used to compare parameters between control and LQTS in the sub group analysis of subjects with QT in the normal range.

3. Results

We did not obtain averaged curves over the entire frequency range (0.9 Hz–1.4 Hz) for all subjects. Accordingly, we have focused our analyses on the data obtained at 1.0 Hz and 1.3 Hz as this combination of frequency bins enabled us to keep the largest number of subjects: 140/159 controls, 133/171 LQTS1 patients and 61/79 LQTS2 patients and include HR dependence into the classifier analyses. A summary of the parameter distributions obtained at all frequencies is provided in the data supplement (supplementary table 1) whilst only the parameter distributions for averaged ECGs recorded at 1.0 Hz and 1.3 Hz are shown in the figures.

3.1. Conventional parameters

An example 1 Hz ECG waveform obtained from a LQTS2 patient is shown in figure 1(a), with the QT, T_h and T_pT_e parameters highlighted. Box and whiskers plots for the values of QT, T_h and T_pT_e at 1.0 Hz and 1.3 Hz are shown in figure 1(b) panels (i)–(iii) respectively. There were statistically significant differences between the three parameters for control, LQTS1 and LQTS2 at both 1.0 and 1.3 Hz. Furthermore, all parameters showed frequency dependences with values for QT, T_h and T_pT_e all lower at 1.3 Hz than at 1.0 Hz. It is also notable that the differences between LQTS1 and LQTS2 are more marked at 1.0 Hz compared to 1.3 Hz.

3.2. Sigmoid parameters

The fitting of the three sigmoid functions to the example LQTS2 ECG T-wave segment is shown in figure 2(a) and summaries of the values for sig int, tau1, tau2 and tau3 are shown as box and whiskers plots in figure 2(b), panels (i)–(iv) respectively. Sig int, which is related to but not identical to QT_p , is significantly longer in LQTS subjects, as expected. A longer tau1 reflects a longer upslope of the T-wave. A longer tau2 reflects a longer downslope and a longer tau3 reflects a slower cross over between the up and down slopes. Tau1, is statistically significantly different between all three groups whereas tau2 and tau3 are similar between control and LQTS1 and only different for LQTS2. Tau1 is also the only one of the three time constants to show a frequency-dependence.

3.3. Polynomial parameters

The fitting of polynomial functions to the upslope and downslopes of the T-wave segments are illustrated in figure 3(a). The polynomial coefficients U_0 and D_0 represent the height of the T-wave at the midpoint of the upslope segment and downslope segments respectively and U_1 , D_1 are the values of the slope of the upslope and downslope at these midpoints. Summaries of the values for max loc, U_0 , U_1 , D_0 and D_1 are shown as box and whiskers plots in figure 3(b), panels (i)–(v) respectively. U_0 and D_0 are both larger for LQTS2 compared to controls or LQTS1. U_0 and D_0 tend to be slightly smaller for LQTS1 compared to controls but this only reaches statistical significance for U_0 at 1.3 Hz. U_1 is smaller in LQTS1 compared to controls whereas it is larger in LQTS2 compared to controls. D_1 is larger (in negative direction) in both LQTS1 and LQTS2 compared to controls. D_1 is close to zero in controls, reflecting the fact

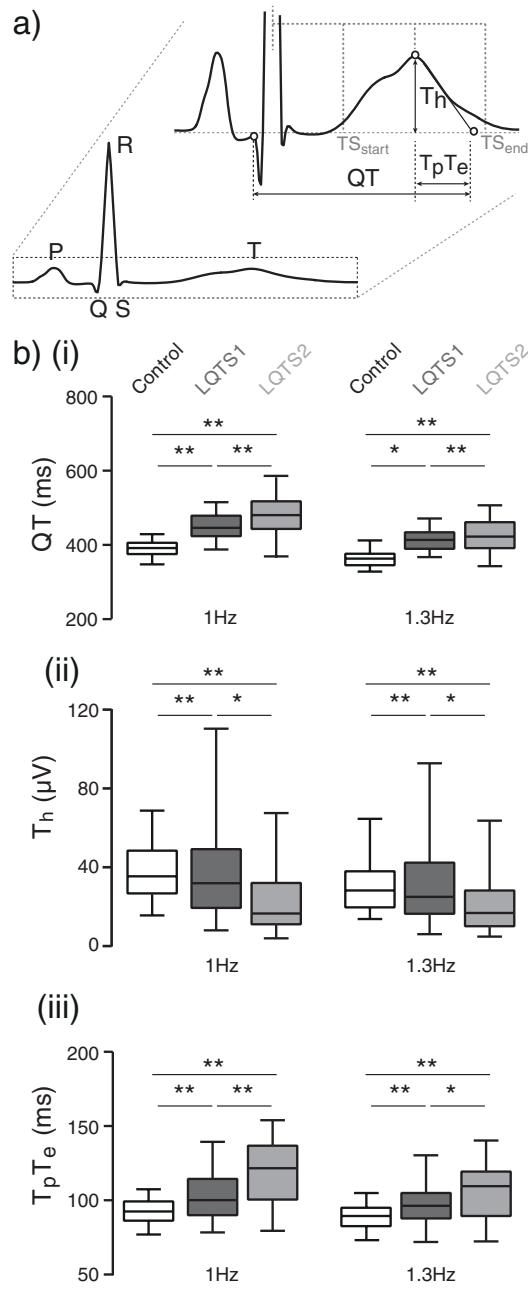


Figure 1. (a) Representative ECG signal from a LQTS2 patient highlighting QT, T_h , and T_pT_e . (b) Box (25–75%) and whisker (5–95%) plots for (i) QT, (ii) T_h , and (iii) T_pT_e values obtained from averaged ECG waveforms for control, LQTS1 and LQTS2 for the 1 Hz and 1.3 Hz binned beats. Lines above box and whisker plots show statistical comparisons with *: $p < 0.01$ and **: $p < 0.001$.

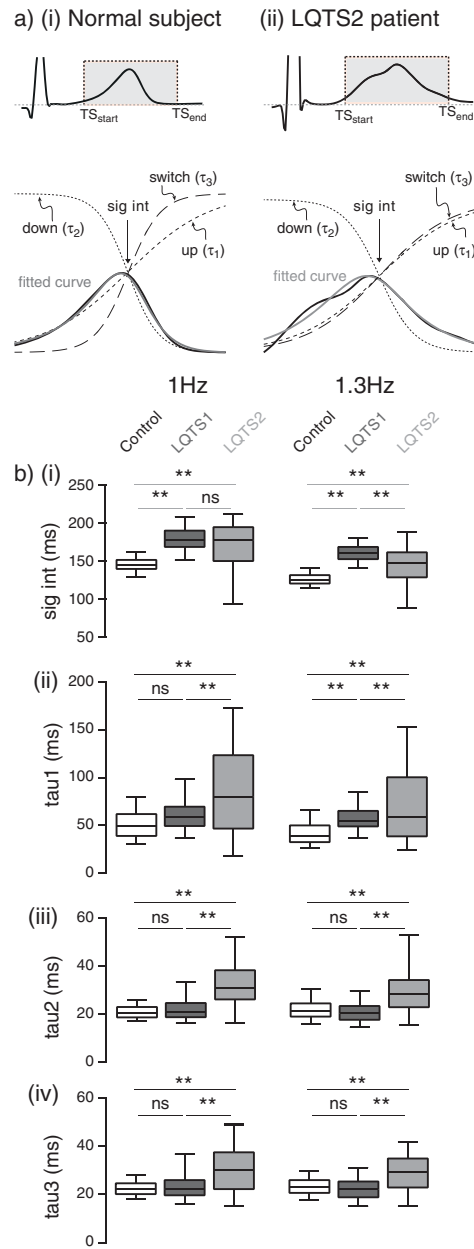


Figure 2. (a) Representative ECG signal from a LQTS2 patient showing the three sigmoidal function fitting on the T wave. Note that the bifid T-wave upstroke is only crudely approximated (grey line) whereas the monotonic downstroke is well fitted by the sigmoidal function fit. (b) Box (25–75%) and whisker (5–95%) plots for (i) sig int, (ii) tau1, (iii) tau2, and (iv) tau3 for control, LQTS1 and LQTS2 at 1 Hz and 1.3 Hz. Lines above box and whisker plots show statistical comparisons with *: $p < 0.01$ and **: $p < 0.001$.

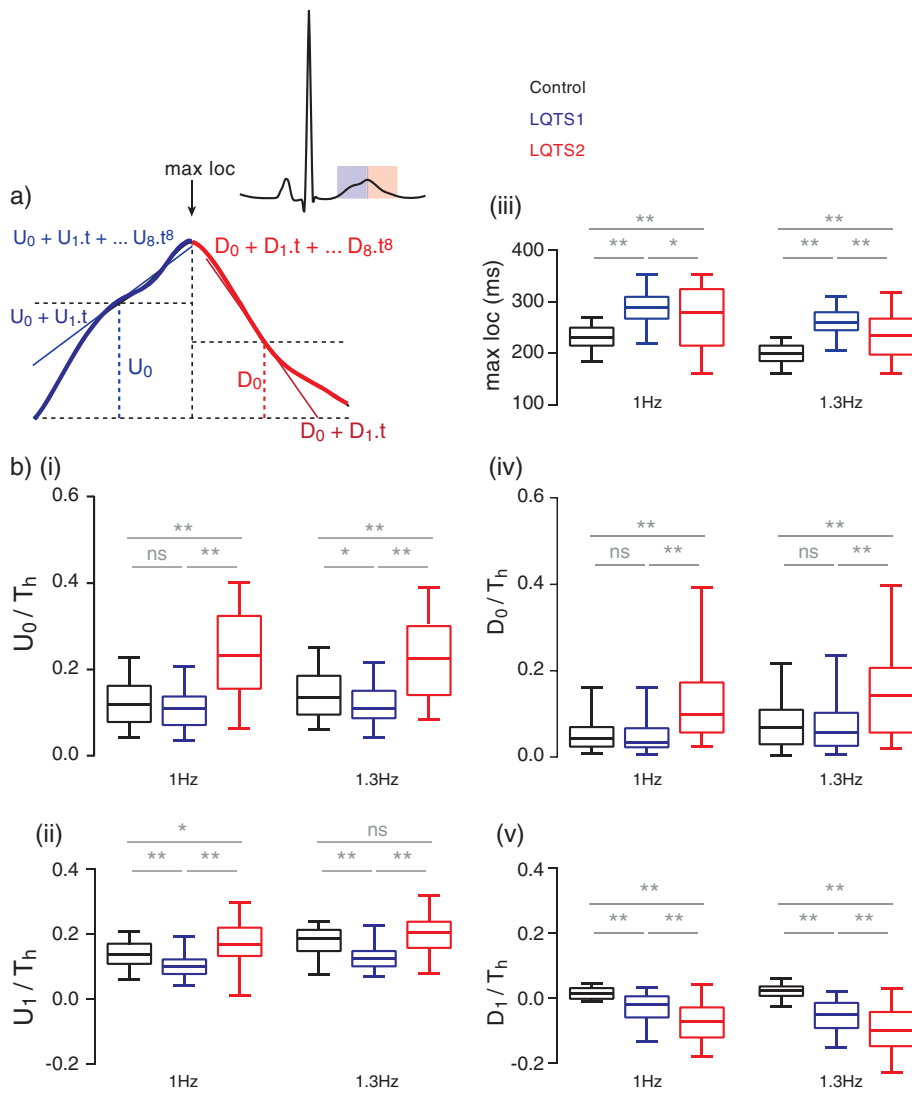


Figure 3. (a) Representative ECG signal from a LQTS2 patient with the T-wave upslope segment and T-wave downslope segments shaded in blue and red respectively. A 9th order polynomial function was fitted to both the upslope and downslope. The t_0 coefficient was defined as the height of the curve at the midpoint of the upslope and downslope segments. Both the bifid T-wave upstroke and the monotonic T wave downstroke are well fitted by 9th order polynomial functions. Also, highlighted are the first two polynomial components (U_0 , U_1 and D_0 , D_1). (b) Box (25–75%) and whisker (5–95%) plots for (i) U_0/T_h , (ii) U_1/T_h , (iii) max loc, (iv) D_0/T_h and (v) D_1/T_h for control, LQTS1 and LQTS2 at 1 Hz and 1.3 Hz. Lines above box and whisker plots show statistical comparisons with *: $p < 0.01$ and **: $p < 0.001$.

that the T-wave has returned to baseline by the midpoint of the analysis window (i.e. it is a flat line). As with the sigmoid functions, polynomial parameters can distinguish between controls and LQTS as well as between LQTS1 and LQTS2.

3.4. Use of T-wave morphology parameters to classify LQTS patients

To investigate whether T-wave morphology markers could improve diagnostic classification of LQTS versus control and between LQTS subtypes, we used a neural network classifier approach as explained in the methods section 2.3. The performance averaged over 100 runs of each classifier type i.e. Control versus LQTS and LQTS1 versus LQTS2 when fed with each parameter group, within each frequency bin is shown in supplementary figure 1. Though most parameters used in our analysis exhibited significant heart rate dependence, it was observed that within each parameter group the classifier performances were not significantly different between the different frequency bins (supplementary figure 1). Hence to maximize the number of subjects with average curves that enter the analysis and at the same time include heart rate dependence of parameters into account, data from frequency bins 1 Hz and 1.3 Hz were utilized in running the classifiers.

Typical example ROC curves for NN classifier outputs based on conventional parameters, sigmoid parameters and polynomial parameters (including data at both 1.0 and 1.3 Hz) are shown in the left panel of figure 4. These curves were chosen because their outputs were close to the mean of 100 runs of the NN classifier algorithm for each group. The averaged NN performance for those 100 runs is shown in the form of confusion matrices in middle panel (Control versus LQTS) and the right panel (LQTS1 versus LQTS2) of figure 4. Classifiers based on sigmoid and polynomial fit based parameters included the Sig int and max loc parameter respectively, which are both related to the QT interval, so we did not include the conventional parameters in the sigmoid or polynomial fit based classifiers.

The classifier based on conventional parameters gave very good discrimination for control versus LQTS but discrimination between LQTS subtypes was not as good, with an average AUC value of 0.800 ± 0.009 (mean \pm SEM). By comparison when we used just QT interval at 1.0 Hz (which is similar to the current clinical practice), we obtained AUC values of 0.82 for control versus LQTS and 0.71 LQTS1 versus LQTS2. The classifiers based on sigmoid and polynomial parameters achieved a similar level of discrimination between control and LQTS as that seen for the classifier based on conventional parameters ($p = 0.19$). However, the sigmoid and polynomial parameter based classifiers were both much better at discriminating between LQTS subtypes than with the conventional parameter based classifier (both $p < 0.0001$). There was no significant difference between the ability of sigmoid parameter based classifier and polynomial parameter based classifier to discriminate between LQTS subtypes.

3.5. Analysis of LQTS genotype-positive patients with normal QT intervals

One of the more difficult problems in the management of suspected LQTS patients is how to determine which patients with a clinical history that sounds like cardiac syncope but who have a normal QT interval on their resting ECG, in fact might have LQTS. To investigate whether our algorithms might help in identifying such patients, we utilized the above designed classifiers to analyze a sub group of patients who had a QT interval in the range of 400–450 ms on their average curves at 1 Hz central frequency. This included 67 controls, 53 LQTS1 patients and 8 LQTS2 patients. Due to the small numbers of LQTS2 patients we only analyzed the groups as control versus LQTS, which is a better reflection of the likely clinical scenario where one does not know what genetic mutation the syndrome may be associated with.

Figure 5 shows distribution of conventional, sigmoid and polynomial parameters in patients with a normal QT interval (400–450 ms) at 1.0 Hz. QT interval was still slightly

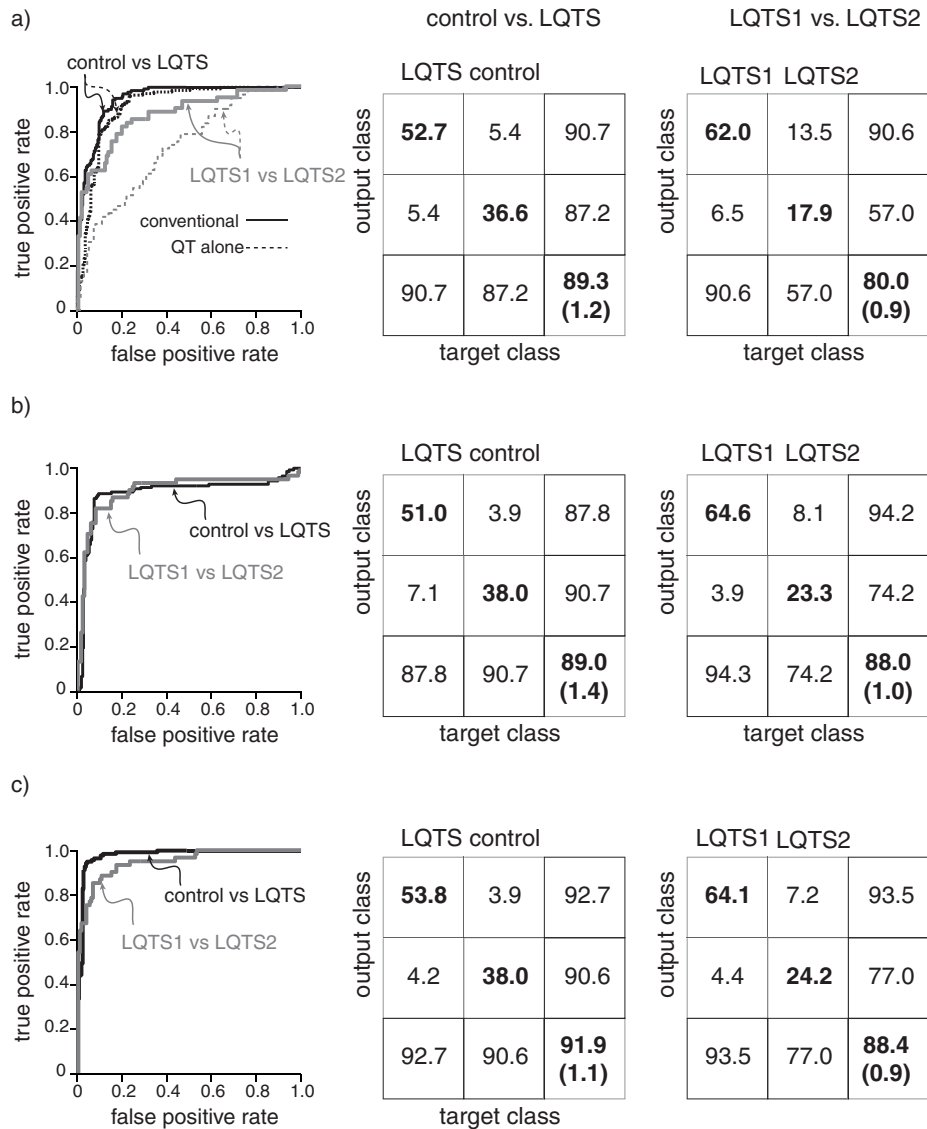


Figure 4. Typical ROC curves (left panel) for classification of control versus LQTS (black) and LQTS1 versus LQTS2 (grey) and summary confusion matrices for classification of control versus LQTS (middle panel) and LQTS1 versus LQTS2 (right panel) using parameters based on (a) all three conventional parameters at both 1.0 and 1.3 Hz (b) parameters derived from sigmoid functions and (c) parameters derived from polynomial functions. Additional ROC curves in top left panel represents classification based on QT at 1 Hz alone (control versus LQTS—black dotted; LQTS1 versus LQTS2—grey dotted). The average percentage classification accuracy from 100 independent runs of each classifier are shown along the left diagonal of each confusion matrix, with the overall accuracy of classification shown as mean ± SEM in the right corner square.

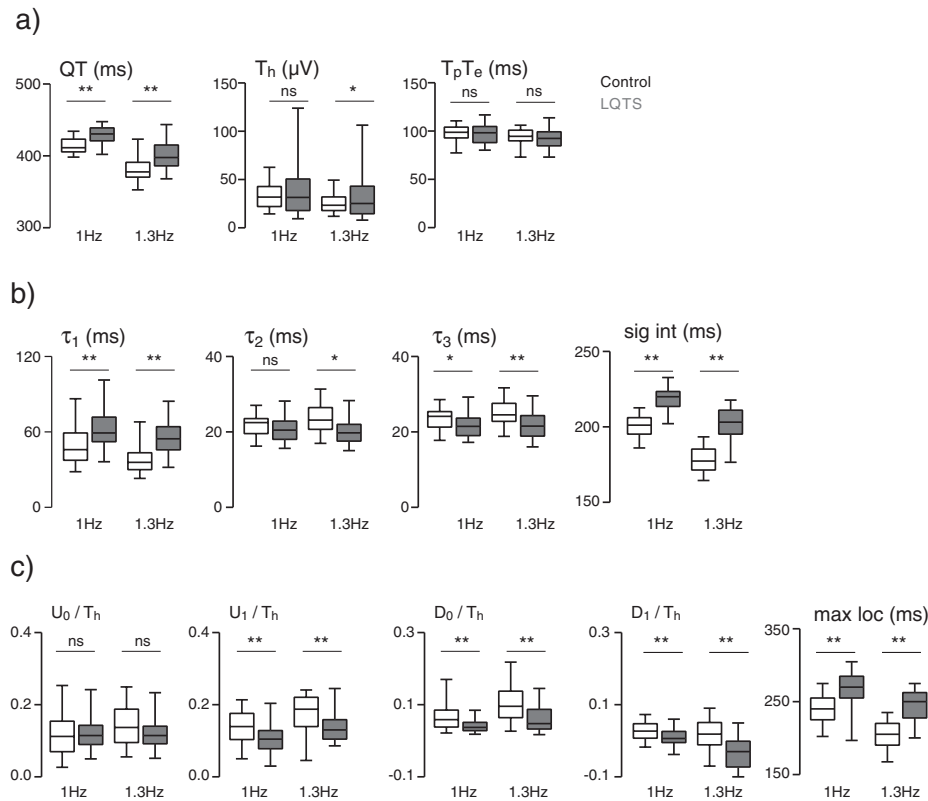


Figure 5. Box (25–75%) and whisker (5–95%) plots for (a) conventional, (b) sigmoid fit and (c) polynomial fit parameters extracted from beats within 1 Hz and 1.3 Hz bins, shown for controls and LQTS subjects (restricted just to those subjects in both groups with QT interval in the range 400–450 ms at 1 Hz central frequency). Lines above box and whisker plots show statistical comparisons with *: $p < 0.01$ and **: $p < 0.001$.

longer in the LQTS group compared to controls but there were no significant difference in T_h or $T_p T_e$ values. τ_1 (both 1 Hz and 1.3 Hz) and τ_3 (1.3 Hz only) were significantly different between control and LQTS patients. U_1 , D_0 and D_1 were all significantly different ($p < 0.01$) between control and LQTS patients whereas U_0 was not (see figure 5).

Example ROC curves and summary confusion matrices for classification of controls versus genotype-positive LQTS patients with normal QT intervals (400–450 ms) are shown in figure 6. The polynomial and sigmoid-based classifiers performed better than the conventional parameter based classifier with AUC values of 0.90 ± 0.01 , 0.90 ± 0.01 and 0.80 ± 0.01 respectively. Mean data for NN classifier accuracy confirms superiority of T-wave morphology based classifiers but there was no significant difference between the sigmoid fit and polynomial fit based approaches. Classifier analysis for controls versus just LQTS1 subjects gave very similar results (data not shown).

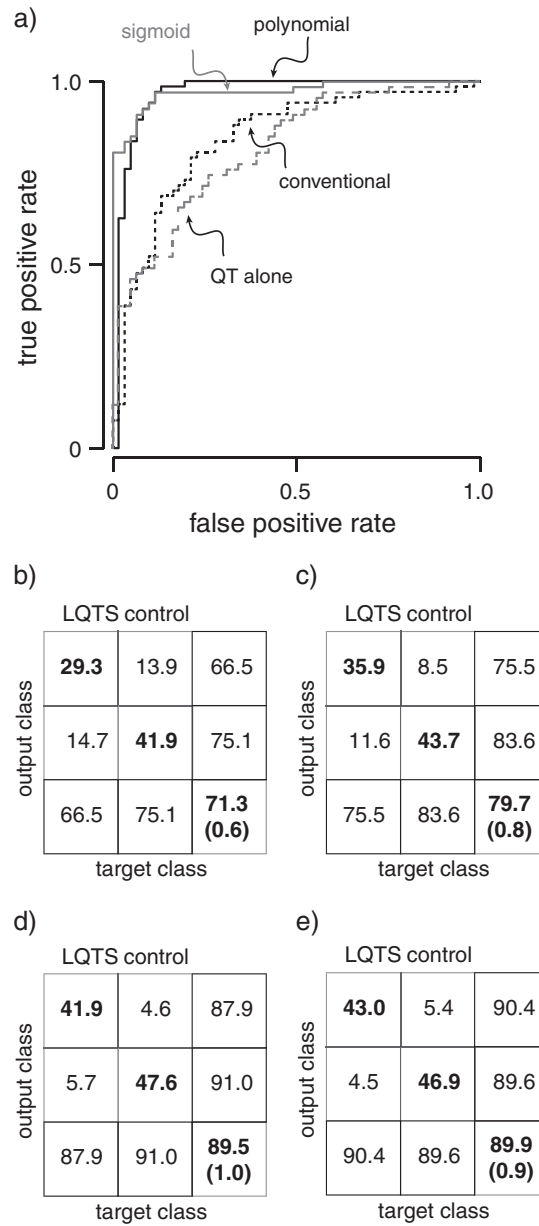


Figure 6. (a) Typical ROC curves for classification of control versus LQTS patients with QT interval in the range 400–450 ms curves at 1 Hz central frequency using QT at 1 Hz alone (grey dotted), conventional (black dotted), sigmoid fit (grey) or polynomial fit (black) parameters. (b) Summary confusion matrices for classification of control versus LQTS patients with QT using conventional (b), sigmoid fit (c) or polynomial fit (d) parameters. The average percentage classification accuracy from 100 independent runs of each classifier are shown along the left diagonal of the confusion matrices, with the overall accuracy of classification shown as mean ± SEM in the right corner square.

4. Discussion

Sudden cardiac death due to cardiac arrhythmias represents the final common end point of abnormal cardiac electrical activity (Wit and Janse 2001) and accounts for ~10% of deaths in the Western world. If we are to reduce the impact of sudden death we need better tools for screening and detection of patients at highest risk. The current paradigm for thinking about cardiac arrhythmias involves the concepts of (i) a substrate, which may be as complex as the scar tissue following multiple myocardial infarctions or as simple as a genetic mutation in a cardiac ion channel, (ii) dynamic factors that can modify the substrate, e.g. changes in adrenergic tone, changes in heart rate and (iii) a trigger that can initiate an arrhythmia if it occurs at a time when the dynamic substrate is conducive for maintenance of an arrhythmia. To improve our ability to stratify risk for lethal cardiac arrhythmias, we need biomarkers that can characterise each of these three components (Hill *et al* 2016).

In this study, we have used LQTS as a proof of concept case for developing tools to characterise pro-arrhythmic substrates. Whilst, measurement of the QT interval is well accepted as a standard clinical marker of repolarization and for diagnosing patients with congenital LQTS, there is a growing body of research suggesting that ECG derived markers based on the T wave morphology can provide additional useful information (Kanters *et al* 2004, Vaglio *et al* 2008). In this study, we have developed automated routines for the analysis of T-wave morphology (as well as conventional ECG parameters) in ECG waveforms derived from Holter ECG recordings and demonstrated that they can significantly enhance the detection of LQTS patients, even when they have a normal QT interval.

Our methodology was focussed towards a fully automated/computerized classification approach utilizing simple T wave slope based parameters applied to Holter data that provides a large set of beats in a range of heart rates. In addition to measuring the traditional features of the surface ECG, including QT interval, T_h (amplitude of the T-wave), and T_pT_e (duration of the descending limb of the T-wave) we have analyzed the morphology of the upslope of the T-wave and down-slope of the T-wave by fitting them with Boltzmann sigmoid functions. Also as a novel approach, polynomial fitting of the T wave upslope and down slope has been included in our methodology. Parameters from both curve-fitting approaches were compared for their ability to discriminate between controls and LQTS patients as well as between subtypes of LQTS syndrome. The polynomial and sigmoidal fitting parameters were comparable to each with both performing better than conventional parameters in differentiating between LQTS1 and LQTS2 patients.

There has been great interest recently in trying to identify more accurate screening tools that could pick up more asymptomatic LQTS individuals. This is because, up to 25% of genotype positive LQTS patients have a normal QT interval (Goldenberg *et al* 2011) and almost 50% of LQTS families are identified subsequent to the death of the proband case. Also, different subsets of LQTS patients have different clinical histories—e.g. many but not all LQTS1 patients have arrhythmias triggered by exercise, especially swimming, and many but not all LQTS2 have arrhythmias triggered by loud noise (Schwartz *et al* 2001). Our results demonstrate the possibility of discriminating LQTS subjects from healthy controls and also distinguishing LQTS patients by genotype using automatic methods that utilize simple measures based on T wave morphology. Especially, within subjects with QT in the normal range (400–450 ms at 1.0 Hz), the accuracy of distinguishing LQTS from control subjects was improved in classifiers based on curve fitting parameters than the ones based on conventional parameters. Between sigmoidal and polynomial fit based approaches, the performances were comparable. Our study shows that the use of simple measurements such as the upslope and downslopes of the T-wave provide good discrimination between both Control versus LQTS and LQTS1 versus LQTS2 subject groups.

Several studies have performed morphological analysis of T waves in relation to diagnosis and classification of LQTS. These studies have used parameters ranging from simple timing components, relative slopes of upslope and downslope components (Couderc *et al* 2006, Kanters *et al* 2008), T-wave asymmetry (Struijk *et al* 2006), repolarization integrals (Kanters *et al* 2004) to complex vector quantities like T wave loop dispersion (Vaglio *et al* 2008). Approaches such as principal component analysis have also been used to study dynamics and complexity of ventricular repolarisation (Perkiomaki *et al* 2002) and in LQTS classification (Dubois *et al* 2012) using multi-lead ECG recordings. These previous studies have achieved comparable discriminatory power, to that reported here, when comparing control versus LQTS patients and for discriminating between LQTS1 and LQTS2 patients. Couderc *et al* (2006), also looked at controls versus LQTS2 patients with borderline QT prolongation (QTc in the range 390–470 ms) and were able to achieve 88% correct classification based on analysis of digitized resting ECGs. This is comparable to the 90% we achieved here (see figure 6) although in our analyses we only included patients with QTc between 400–450 ms and our cohort of LQTS patients with normal QT interval consisted primarily of LQTS1 patients.

The long-term aim of our work is to develop automated tools that can enable more accurate quantification of risk for lethal cardiac arrhythmias. Our results to date represent progress in identifying biomarkers that can quantify pro-arrhythmic substrates. Beyond that however we still need to investigate how these biomarkers may be influenced by dynamic factors known to modify pro-arrhythmic substrate, e.g. changes in adrenergic tone and changes in heart rate. In this regard, we have already shown that many of the novel parameters studied here are influenced by heart rate when applied to waveforms averaged over several hundreds beats. We anticipate that similar changes will be observed when analysed on a beat-by-beat basis. This however will involve intense computational tasks. Nevertheless, numerous groups have started to develop sophisticated tools to analyse Holter ECG recordings for beat-to-beat dynamics of repolarization (Berger *et al* 1997, Zauneder *et al* 2014, Baumert *et al* 2016, Page *et al* 2016) and in the future we propose to combine these techniques with our novel biomarkers to investigate whether they provide more insights into the dynamic nature of pro-arrhythmic substrates in patients with LQTS.

4.1. Limitations

Despite the promising results in this study, there are also some important limitations that will need to be addressed before we can start to apply such techniques clinically. In this study, we have utilized a beat binning approach. This has the advantage of improving the signal-noise ratio by averaging multiple beats. However, following a change in heart rate it takes many beats before the QT interval and the T-wave morphology fully adapt to the new heart rate. As we did not differentiate between beats that occur against a background of an increasing heart rate or a decreasing heart rate our beat-binned averaged waveforms will be an approximation of a typical ECG waveform at that heart rate (Malik 2005). Whilst the improved signal to noise greatly facilitates the curve fitting process, it is likely that we will have missed some subtle features within each waveform. In addition we have not taken into account a number of confounding factors that could influence our results. For example, we have not taken into account, the influence of gender or age in our analyses (Surawicz and Parikh 2003), nor separated groups based on use of beta-blockers. The simple reason for this was lack of sample size. It is also possible that we may have introduced some bias in our patient selection as we eliminated patients with inverted T-waves and our ‘visual inspection’ criteria will have eliminated cases

that had the smallest amplitude T-waves. Thus it will be important to investigate whether the discriminatory power of our algorithms can be replicated in an independent cohort of patients. Despite these limitations, our results are very encouraging and confirm prior work demonstrating the interest and utility of considering T-wave morphology in the analysis of the body surface ECGs from patients suspected of carrying LQTS mutations.

5. Conclusion

Analysis of T-wave morphology in frequency binned averaged ECG signals obtained from 24h Holter recordings can differentiate between genotype confirmed LQTS subtypes. Also, we can separate healthy controls and LQTS patients with normal QT intervals. The findings support the claim that more intensive analysis of ECG phenotypes has the potential to identify and sub-stratify patients with pro-arrhythmic substrates. Feasibility of our approach provides an incentive to acquire larger cohorts and to further develop the technology to apply neural network classifiers as well as other approaches including machine learning approaches and principal component analysis on multi lead ECG data so that we can better discriminate between high and low risk patients.

Acknowledgments

This work was supported by grants from the National Health and Medical Research Council of Australia (App 1074386 to JIV), funds from the Office of Health and Medical Research, NSW State Government and the St Vincent's clinic Foundation. JV is supported by an NHMRC Senior Research Fellowship. Patient data used for this research were provided by the Telemetric and Holter ECG Warehouse (THEW) of the University of Rochester.

References

- Badilini F, Maison-Blanche P, Childers R and Coumel P 1999 QT interval analysis on ambulatory electrocardiogram recordings: a selective beat averaging approach *Med. Biol. Eng. Comput.* **37** 71–9
- Badilini F, Vaglio M, Dubois R, Roussel P, Sarapa N, Denjoy I, Extramiana F and Maison-Blanche P 2008 Automatic analysis of cardiac repolarization morphology using Gaussian mesa function modeling *J. Electrocardiol.* **41** 588–94
- Baumert M 2016 Measurement of T wave variability in body surface ECG *J. Electrocardiol.* in press
- Baumert M *et al* 2016 QT interval variability in body surface ECG: measurement, physiological basis, and clinical value: position statement and consensus guidance endorsed by the European heart rhythm association jointly with the ESC working group on cardiac cellular electrophysiology *Europace* **18** 925–44
- Berger R D, Kasper E K, Baughman K L, Marban E, Calkins H and Tomaselli G F 1997 Beat-to-beat QT interval variability novel evidence for repolarization lability in ischemic and nonischemic dilated cardiomyopathy *Circulation* **96** 1557–65
- Bhuiyan T A, Graff C, Kanters J K, Nielsen J, Melgaard J, Matz J, Toft E and Struijk J J 2015 The T-peak–T-end Interval as a marker of repolarization abnormality: a comparison with the QT interval for five different drugs *Clin. Drug Investig.* **35** 717–24
- Couderc J-P 2010 A unique digital electrocardiographic repository for the development of quantitative electrocardiography and cardiac safety: the telemetric and Holter ECG warehouse (THEW) *J. Electrocardiol.* **43** 595–600
- Couderc J-P, McNitt S, Xia J, Zareba W and Moss A J 2006 Repolarization morphology in adult LQT2 carriers with borderline prolonged QTc interval *Heart Rhythm* **3** 1460–6

- Couderc J-P, Zareba W, Moss A J, Sarapa N, Morganroth J and Darpo B 2003 Identification of sotalol-induced changes in repolarization with T wave area-based repolarization duration parameters *J. Electrocardiol.* **36** 115–20
- Dubois R, Extramiana F, Denjoy I, Maison-Blanche P, Vaglio M, Roussel P, Babilini F and Leenhardt A 2012 A machine learning approach for LQT1 versus LQT2 discrimination *IEEE Comput. Cardiol.* pp 437–40
- Goldenberg I et al 2011 Risk for life-threatening cardiac events in patients with genotype-confirmed long-QT syndrome and normal-range corrected QT intervals *J. Am. Coll. Cardiol.* **57** 51–9
- Goldenberg I, Moss A J and Zareba W 2006 QT interval: how to measure it and what is normal *J. Cardiovasc. Electrophysiol.* **17** 333–6
- Goldenberg I, Zareba W and Moss A J 2008 Long QT syndrome *Curr. Probl. Cardiol.* **33** 629–94
- Hill A P et al 2016 Computational cardiology and risk stratification for sudden cardiac death: one of the grand challenges for cardiology in the 21st century *J. Physiol.* in press
- Hodkinson E C et al 2016 Heritability of ECG Biomarkers in the Netherlands twin registry measured from Holter ECGs *Front. Physiol.* **7** 154
- Kanters J K et al 2008 T peak T end interval in long QT syndrome *J. Electrocardiol.* **41** 603–8
- Kanters J K, Fanoe S, Larsen L A, Thomsen P E B, Toft E and Christiansen M 2004 T wave morphology analysis distinguishes between KvLQT1 and HERG mutations in long QT syndrome *Heart Rhythm* **1** 285–92
- Katritsis D G, Siontis G C and Camm A J 2013 Prognostic significance of ambulatory ECG monitoring for ventricular arrhythmias *Prog. Cardiovasc. Dis.* **56** 133–42
- Lehmann M H, Suzuki F, Fromm B S, Frankovich D, Elko P, Steinman R T, Fresard J, Baga J J and Taggart R T 1994 T wave ‘humps’ as a potential electrocardiographic marker of the long QT syndrome *J. Am. Coll. Cardiol.* **24** 746–54
- Malik M 2005 Assessment of drug-induced QT prolongation: to bin or not to bin? *Clin. Pharmacol. Ther.* **4** 241–6
- Mauriello D A, Johnson J N and Ackerman M J 2011 Holter monitoring in the evaluation of congenital long QT syndrome *Pacing Clin. Electrophysiol.* **34** 1100–4
- Moss A and Robinson J 1992 Clinical features of the idiopathic long QT syndrome *Circulation* **85** 1140–4
- Moss A J and Schwartz P J 2005 25th anniversary of the international long-QT syndrome registry an ongoing quest to uncover the secrets of long-QT syndrome *Circulation* **111** 1199–201
- Padrini R, Butrous G, Camm A and Malik M 1995 Algebraic decomposition of the TU wave morphology patterns *Pacing Clin. Electrophysiol.* **18** 2209–15
- Page A, Aktas M K, Soyata T, Zareba W and Couderc J-P 2016 ‘QT clock’ to improve detection of QT prolongation in long QT syndrome patients *Heart Rhythm* **13** 190–8
- Perkiomaki J S, Zareba W, Nomura A, Andrews M, Kaufman E S and Moss A J 2002 Repolarization dynamics in patients with long QT syndrome *J. Cardiovasc. Electrophysiol.* **13** 651–6
- Rosen M R 2002 The electrocardiogram 100 years later electrical insights into molecular messages *Circulation* **106** 2173–9
- Schwartz P J et al 2001 Genotype-phenotype correlation in the long-QT syndrome gene-specific triggers for life-threatening arrhythmias *Circulation* **103** 89–95
- Splawski I et al 2000 Spectrum of mutations in long-QT syndrome genes KVLQT1, HERG, SCN5A, KCNE1, and KCNE2 *Circulation* **102** 1178–85
- Struijk J J, Kanters J K, Andersen M P, Hardahl T, Graff C, Christiansen M and Toft E 2006 Classification of the long-QT syndrome based on discriminant analysis of T-wave morphology *Med. Biol. Eng. Comput.* **44** 543–9
- Surawicz B and Parikh S R 2003 Differences between ventricular repolarization in men and women: description, mechanism and implications *Ann. Noninvasive Electrocardiol.* **8** 333–40
- Task Force of The European Society of Cardiology and The North American Society of Pacing and Electrophysiology 1996 Heart rate variability: standards of measurement, physiological interpretation and clinical use *Circulation* **93** 1043–65
- Vaglio M, Couderc J-P, McNitt S, Xia X, Moss A J and Zareba W 2008 A quantitative assessment of T-wave morphology in LQT1, LQT2, and healthy individuals based on Holter recording technology *Heart Rhythm* **5** 11–8
- Vincent G M 2005 Risk assessment in long QT syndrome: the Achilles heel of appropriate treatment *Heart Rhythm* **2** 505–6
- Wit A L and Janse M J 2001 Reperfusion arrhythmias and sudden cardiac death a century of progress toward an understanding of the mechanisms *Circ. Res.* **89** 741–3

- Zabel M, Malik M, Hnatkova K, Papademetriou V, Pittaras A, Fletcher R D and Franz M R 2002 Analysis of T-wave morphology from the 12-lead electrocardiogram for prediction of long-term prognosis in male US veterans *Circulation* **105** 1066–70
- Zareba W, Couderc J, Moss A, Olsson S, Amlie J and Yuan S 2000 Automatic detection of spatial and temporal heterogeneity of repolarization *Dispersion of ventricular repolarization: State of the Art* (Armonk, NY: Futura Publishing Company, Inc.) pp 85–107
- Zareba W and De Luna A B 2005 QT dynamics and variability *Ann. Noninvasive Electrocardiol.* **10** 256–62
- Zaunseder S, Schmidt M, Malberg H and Baumert M 2014 Measurement of QT variability by two-dimensional warping *2014 8th Conf. of the European Study Group on Cardiovascular Oscillations (ESGCO)* (IEEE) pp 163–4
- Zipes D P *et al* 2006 ACC/AHA/ESC 2006 guidelines for management of patients with ventricular arrhythmias and the prevention of sudden cardiac death: a report of the American College of Cardiology/American Heart Association Task Force and the European Society of Cardiology Committee for Practice Guidelines (writing committee to develop guidelines for management of patients with ventricular arrhythmias and the prevention of sudden cardiac death) *J. Am. Coll. Cardiol.* **48** e247–346